

Asymptotic analysis of dielectric coaxial fibers

Yong Xu, Reginald K. Lee, and Amnon Yariv

Department of Applied Physics, California Institute of Technology, MS 128-95, Pasadena, California 91125

Received January 28, 2002

Using an asymptotic analysis, we analytically calculate the dispersion and the field distribution of guided modes in an all-dielectric coaxial fiber. We compare the analytical results with those obtained from numerical calculations and find excellent agreement between them. We demonstrate that both the Bragg reflection and the total internal reflection play important roles in providing confinement and determining the dispersion characteristics of the coaxial fiber modes. © 2002 Optical Society of America

OCIS codes: 060.4510, 230.1480, 230.7370.

Recently much effort has been devoted to utilizing Bragg reflection to guide light in optical fibers.^{1–6} A particularly appealing application of Bragg confinement is the unique possibility of guiding light in air, which can lead to lower propagation loss and reduce the threshold for nonlinear effects. Such a possibility was first pointed out in Bragg fibers.¹ Other possible candidates for guiding light in air are air-core photonic crystal fibers.^{2,3} Recently, using all-dielectric coaxial fibers to transmit optical signals was suggested.⁴ As shown in Fig. 1(a), the coaxial fiber consists of a low-index coaxial region bounded by a high-index core and a cylindrical omnidirectional mirror. The omnidirectional mirrors, which are Bragg stacks with a large enough index contrast, can be designed so that there is a frequency range within which light that is incident from the low-index medium is completely reflected back, irrespective of the incident angle and polarization.⁷ Thus an analogy can be drawn between dielectric coaxial fibers and metallic coaxial cables. Ibanescu *et al.* identified two single-mode windows for the TM band in a coaxial fiber and predicted a point of zero dispersion.⁴ Such a TM band is truly single mode, in contrast with the fundamental mode of conventional optical fibers, which is always doubly degenerate, and can be used to eliminate completely many undesirable polarization-dependent effects, such as polarization mode dispersion.⁴ However, there is some fundamental difference between the omnidirectional mirrors and the metals. Such a difference may impose limitations on the applications of the coaxial fibers in telecommunications and is studied in this Letter.

We take one of the coaxial fibers studied by Ibanescu *et al.*⁴ as an example and use the asymptotic formalism to study its dispersion properties. In the asymptotic approach,^{5,6} we use the exact solutions of Maxwell equations to describe the fields within the several inner core layers, whereas in the cladding region the exact solutions are approximated in the asymptotic limit, and the guided coaxial fiber modes are found by matching of the transverse field components at the core–cladding interface [the dashed circle in Fig. 1(a)]. The parameters of the coaxial fiber are given in the caption of Fig. 1. The asymptotic results are shown in Fig. 2(a) as thick solid curves, where each photonic

band is labeled according to its angular momentum m : a TE band ($m = 0$), a TM band ($m = 0$), and two $m = 1$ bands. We notice that the TE band was missed in the results by Ibanescu *et al.*⁴ We also use a two-dimensional finite-difference time-domain (FDTD) algorithm⁸ to verify the validity of our asymptotic calculations, and the FDTD results are shown in Fig. 2 as filled circles. In our FDTD calculations, we choose the grid size such that Λ , the total thickness of a Bragg cladding pair, takes 24 FDTD cells. The perfectly matched layer boundary condition⁹ is used to simulate the open space around the coaxial fiber and absorb all the outgoing radiation. We use a discrete Fourier transform to transfer the time-domain data into the frequency domain and extract the frequency of the guided coaxial fiber modes,¹⁰ with frequency resolution of approximately 0.8%. The asymptotic results agree well with the FDTD calculations, which demonstrates the validity of the asymptotic method. The shaded region in Fig. 2(a) corresponds to the TM cladding modes that can propagate in the cylindrical omnidirectional reflector.

If we take out the Bragg cladding of the coaxial fiber, the center dielectric core resembles a conventional optical fiber. Thus, even without the Bragg cladding, the high-index core of the coaxial fiber as studied in Fig. 2(a) supports confined propagating

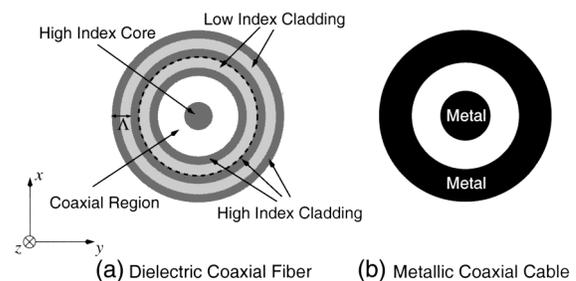


Fig. 1. (a) Cross section of a dielectric coaxial fiber. For the high-index cladding medium, we choose $n_{cl}^1 = 4.6$ and $l_{cl}^1 = (1/3)\Lambda$, whereas for the low-index cladding medium $n_{cl}^2 = 1.6$ and $l_{cl}^2 = (2/3)\Lambda$. Λ is the total thickness of the Bragg cladding pair. For the center core and the coaxial region, we choose $n_{co} = 4.6$ and $l_{co} = 0.4\Lambda$ and $n_{coax} = 1$ and $l_{coax} = 1.0\Lambda$, respectively. (b) Cross section of a metallic coaxial cable.

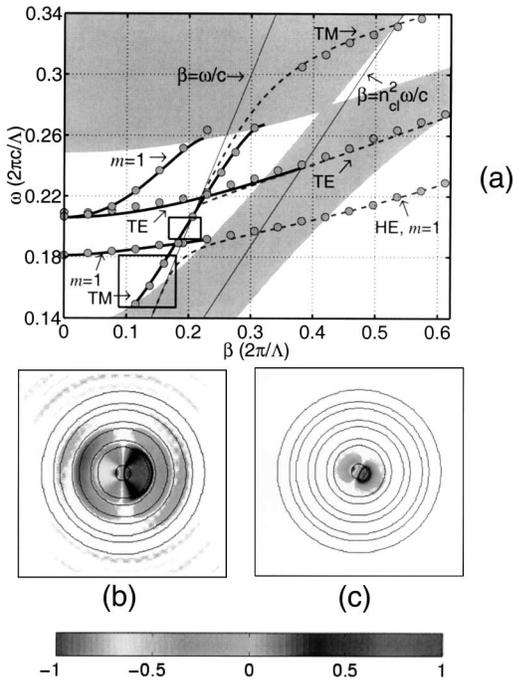


Fig. 2. (a) Dispersion of the coaxial fiber defined in the caption of Fig. 1. The shaded region indicate the existence of propagating TM cladding modes in the omnidirectional reflector. The thick solid curves are results obtained from asymptotic analysis. The filled circles represent the two-dimensional FDTD results. The center core of the coaxial fiber resembles a conventional optical fiber and supports three guided modes: HE, TE, and TM modes. Their dispersions are shown as dashed curves. The single-mode windows for the TM band are illustrated in the figure as two boxes. (b) H_z field distributions of the lower $m = 1$ band at $\beta = 0.153(2\pi/\Lambda)$ and $\omega = 0.187(2\pi c/\Lambda)$. (c) H_z field distributions of the lower $m = 1$ band at $\beta = 0.611(2\pi/\Lambda)$ and $\omega = 0.229(2\pi c/\Lambda)$. In (b) and (c), the field distributions are normalized relative to the maximum H_z value. The scale bar indicates the relative values of the H_z fields in (b) and (c).

modes, and the dispersion of such conventional fiber modes is also shown in Fig. 2(a) as dashed curves. Comparing the conventional fiber dispersion with the FDTD calculations of the full coaxial fiber, we find excellent correspondence between the two for the region below the air light line $\beta = \omega/c$. This strongly suggests that once the guided coaxial fiber modes pass through the air light line the main confining mechanism is actually provided by the center high-index core. To illustrate this point more clearly, we show two FDTD calculations of field distribution of the lower $m = 1$ band. The $m = 1$ mode in Fig. 2(b) has $\beta = 0.153(2\pi/\Lambda)$ and $\omega = 0.187(2\pi c/\Lambda)$ and belongs to the TM bandgap above the air light line. For any modes above the light line, guiding cannot be achieved through total internal reflection, and therefore we observe a substantial field distribution in both the coaxial region (air) and the Bragg cladding. The $m = 1$ mode in Fig. 2(c) has $\beta = 0.611(2\pi/\Lambda)$ and $\omega = 0.229(2\pi c/\Lambda)$ and is below the air light line. As expected, the guided coaxial fiber mode becomes essentially the HE mode of a conventional fiber, with

optical fields mostly confined in the center dielectric core. The two $m = 1$ modes are doubly degenerate and possess mirror reflection symmetry, as can be seen from Figs. 2(b) and 2(c). However, because of the rotational symmetry of the dielectric structure, the plane of mirror reflection symmetry is not unique, and the different mirror reflection symmetry plane in Figs 2(b) and 2(c) is attributed to the initial condition of the FDTD simulations.

In telecommunications applications, it is important to determine the condition of single-mode operation. For the TM mode of the coaxial fiber in this Letter, the lower single-mode frequency window simply contains all the TM modes below the cutoff frequency of the lower $m = 1$ band. As the lower $m = 1$ band enters the shaded region in Fig. 2(a), the TM field component loses confinement in the Bragg cladding, and the $m = 1$ band is no longer a well-defined guided mode. Thus, the second single-TM-mode window begins at the lower intersection of the $m = 1$ band and the TM gap and ends at the smallest of the following frequencies: the cutoff frequency of the higher $m = 1$ band, the cutoff frequency of the TE band, or the higher intersection point of the lower $m = 1$ band and the TM gap where the lower $m = 1$ band enters the TM gap again. The two single-frequency windows are shown in Fig. 2 as two boxes.

In Fig. 3(a), we normalize the TM coaxial band near $1.55 \mu\text{m}$ and calculate dispersion parameter D ,

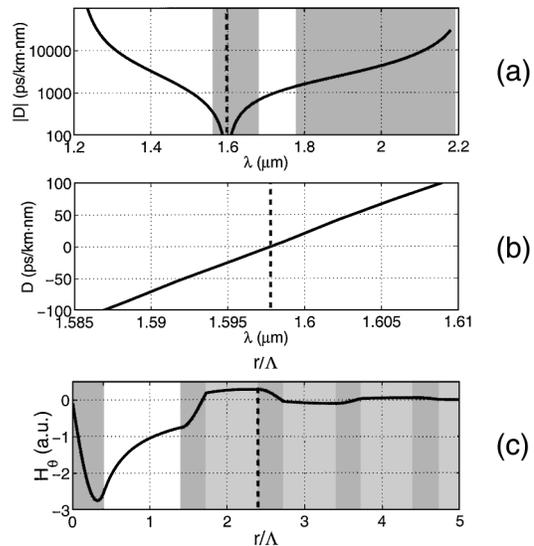


Fig. 3. (a) Absolute value of dispersion parameter D of the coaxial fiber TM band. Wavelength λ is normalized such that the TM band crosses air light line $\beta = \omega/c$ at $1.55 \mu\text{m}$. At $\lambda = 1.598 \mu\text{m}$ [or $\omega = 0.202(2\pi c/\Lambda)$], dispersion parameter D becomes zero, which is shown as the dashed line. The two single-mode windows in Fig. 2 are shown as shaded regions. To the left of the dashed line, D is negative, whereas D is positive to the right of the dashed line. (b) Dispersion parameter D within the vicinity of $D = 0$. (c) H_θ field of the TM coaxial fiber mode at $D = 0$. The unshaded, light, and dark regions represent air ($n_{\text{coax}} = 1$), the low-index dielectric medium ($n_{\text{cl}}^2 = 1.6$), and the high-index dielectric medium ($n_{\text{cl}}^1 = 4.6$), respectively.

which is defined as $(2\pi c/\lambda^2)(d^2\beta/d\omega^2)$, from the asymptotic results. The two single-frequency windows are identified in Fig. 3(a) by the shaded region. We immediately notice that dispersion parameter D takes a very large value at most frequencies and can be either positive or negative. Near $1.6 \mu\text{m}$, D crosses the point of zero dispersion but remains small only within a small frequency range. Ibanescu *et al.* predicted a point of zero dispersion⁴ but did not give the frequency of the zero dispersion point. Our results in Fig. 3(b) confirm their prediction, yet at the same time we notice that the frequency window of small D is too small for optical signal transmission in telecommunications. Using the asymptotic analysis, we also calculate the H_θ component of the TM mode at the zero dispersion frequency $\omega = 0.202(2\pi c/\Lambda)$ and show the results in Fig. 3(c). From Fig. 3(c), it is obvious that there is a substantial presence of an electromagnetic field in the high-index core. As a result, using this coaxial fiber mode to guide light does not provide much benefit in terms of reducing material absorption and nonlinear effects. The substantial presence of field in the high-index core also illustrates that the analogy between dielectric coaxial fibers and metallic coaxial cables is not perfect. Turning our attention to the cladding field, we find that the field strength in the first cladding pairs, even though it is relatively small, is not negligible. In fact, the fields in the first Bragg pair cannot be neglected, since optical fields must penetrate at least one cladding pair to experience Bragg confinement. The existence of the cladding field also explains the large modal dispersion that we find in Fig. 3(a), since any guided coaxial fiber mode must “feel” three different dielectric media: air in the coaxial region, the high-index cladding, and the low-index cladding.

In conclusion, we have applied an asymptotic formalism to analyze the dispersion of a dielectric coaxial fiber. The dielectric coaxial fibers provide the interesting possibility of truly single-mode guiding instead of conventional guiding, which is always provided by doubly degenerate modes. We find that both Bragg reflection and total internal reflection play an important role in determining modal dispersion of the coaxial fiber, in contrast with other conventional fibers in which only one of the two guiding mechanisms

provides confinement. Such a mixture of guiding mechanisms may provide interesting possibilities in engineering photonic band structures and dispersion properties. From our asymptotic analysis, we find that the analogy between dielectric coaxial fibers and a metallic coaxial cable is not entirely accurate, and there are a substantial number of optical fields in the high-index core and the Bragg cladding, which results in large dispersion for guided coaxial fiber modes. The large modal dispersion is undesirable for long distance telecommunications yet may be of great interest for other applications in which large dispersion is required. Finally, even though the coaxial guiding region in our analysis is taken to be air, which would be difficult to realize, in reality the coaxial region can be made from materials with low refractive indices, and the main observations of this Letter will still apply.

This research was sponsored by the U.S. Office of Naval Research, whose support is gratefully acknowledged. Y. Xu's e-mail address is yong@its.caltech.edu.

References

1. P. Yeh, A. Yariv, and E. Marom, *J. Opt. Soc. Am.* **68**, 1196 (1978).
2. J. C. Knight, J. Broeng, T. A. Birks, and P. St. J. Russell, *Science* **282**, 1476 (1998).
3. R. F. Cregan, B. J. Mangan, J. C. Knight, T. A. Birks, P. St. J. Russell, P. J. Roberts, and D. C. Allan, *Science* **285**, 1537 (1999).
4. M. Ibanescu, Y. Fink, S. Fan, E. L. Thomas, and J. D. Joannopoulos, *Science* **289**, 415 (2000).
5. Y. Xu, R. K. Lee, and A. Yariv, *Opt. Lett.* **25**, 1756 (2000).
6. Y. Xu, G. X. Ouyang, R. K. Lee, and A. Yariv, *J. Light-wave Technol.* **20**, 428 (2002).
7. Y. Fink, J. N. Winn, S. Fan, C. Chen, J. Michel, J. D. Joannopoulos, and E. L. Thomas, *Science* **282**, 1679 (1998).
8. F. Zepparelli, P. Mezzanotte, F. Alimenti, L. Roselli, R. Sorrentino, G. Tartarini, and P. Bassi, *Opt. Quantum Electron.* **31**, 827 (1999).
9. S. D. Gedney, *IEEE Trans. Antennas Propag.* **44**, 1630 (1996).
10. C. M. Furse and O. P. Gandhi, *IEEE Microwave Guided Wave Lett.* **5**, 326 (1995).